Electrochemical and Metallurgical Behavior of Lead-Magnesium Casting Alloys as Grids for Lead-Acid Batteries

Salma Khatbi*, Youssef Gouale, Abdeslam Lamiri and Mohamed Essahli

Univ. Hassan 1, Laboratory of Applied Chemistry and Environment, Faculty of Science and Technology, BP 5777, Settat, Morocco

*Corresponding author: khatbisalma@gmail.com

Received September, 3, 2018; accepted November 8, 2020
https://doi.org/10.4152/pea.2021390403

Abstract

In order to evaluate the influence of magnesium on the corrosion resistance of lead anodes in H_2SO_4 4 M, as well as on the microcrystalline morphology of lead, different electrochemical and metallurgical studies were made, such potentiodynamique polarization, electrochemical impedance spectroscopy, microhardness evolution, X-ray fluorescence spectroscopy and optical microscopy. The obtained results have shown that the addition of magnesium up to 1.5% in weight leads to a significant decrease in the corrosion current density (I_{corr}) and therefore, it increases the corrosion inhibition efficiency to 83% and it reduces the famous sulfation phenomena, by facilitating the transformation of $PbSO_4$ and PbO to PbO_2. It also makes the micro-structure of Pb much stronger, which makes the Pb anodes more resistant to mechanical shocks within the battery. We have also studied the effect of temperature on the corrosion of the new casting alloys. We found that an increase in temperature led to a decrease in its effect on the corrosion of alloys, compared with that of pure lead. Therefore, the new improved battery is more resistant, durable and more environment friendly.

***Keywords**:* battery, corrosion, Pb-Mg, electro-chemistry.

Introduction

Pure lead is too fragile to be used alone in the batteries; it corrodes easily by being immersed in 4 M sulfuric acid. Within the battery, the anode of pure lead will lengthen and deform, which makes the layer of PbO_2 crack, exposing it to oxidation and also to an accelerated corrosion, which has been proven by A. Felder and R. D. Prengaman [1]. The lead-acid batteries also suffer from the sulfation phenomenon, which is the formation of $PbSO_4$ covering the surface of lead and preventing the electrochemical reactions to occur, thus reducing the length of the battery life [2]. It is for these reasons that a lot of researches have recently been made to develop some alloys based on lead, which have better corrosion resistance and better hardness, allowing the battery to last longer. Some researchers have chosen to add some chemical products into the electrolyte of the battery, e.g., there are phosphorus compounds, such as phosphoric acid and its

salts, which have given some very remarkable results, when it comes to decrease the appearance of the sulphation phenomenon [3-5].
Many researches have recently been made to find the best alloys capable of replacing the pure lead plates. Wislei R. Osorio et al [6] have found that the Pb-1% Sn and Pb-2.5% Sn alloys immersed in 0.5 M H_2SO_4 considerably reduce lead corrosion, when these alloys have coarse grains, in comparison with other alloys that have finer grains. Also, this type of alloys allows to make much lighter batteries. M. I. Cˇekerevac et al [7] and R. David Prengaman [8] have studied the influence of the addition of tin and silver on Pb corrosion rate, by modifying its micro-structure. They have found that, indeed, the Pb-Ca-Sn-Ag alloy is more resistant to corrosion, in comparison with pure Pb, and that by increasing the concentration of the added Sn and Ag, the micro-structure of the primary alloy Pb-Ca is modified in a positive way. L. Albert and Al [9] have found that, when Sn is added up to 1.2% in weight, the passivation rate of the Pb-Ca-Sn alloys decrease, under conditions that simulate the deep discharge of the battery, by increasing the conductivity of the PbO layer that is usually formed on the metal surface. Very little researches have been done to evaluate the effect of the addition of aluminum on lead corrosion in batteries, and, for this reason, we chose aluminum to be our element of addition.
Prior to this work, we assessed the effect of the addition of chemical compounds containing phosphorus on lead corrosion, and it has been proved that these elements significantly reduce lead corrosion rate in batteries [11]. We also studied the electrochemical and metallurgical effect of aluminum on lead corrosion in 4 M H_2SO_4; we found that aluminum added up to 1.5% in weight leads to an increase in the micro-hardness of Pb-Al alloys, reduces the corrosion current density (I_{corr}) and decreases Pb corrosion rate by 51.15% [12].
Therefore, the present work focused on a new alloy that has never been investigated for the improvement of the lead-acid battery. We chose to study the effect of Mg content on certain mechanical properties, e.g., micro-hardness, micro-structural, electrochemical and corrosion behaviour of synthetic Pb-Mg alloys prepared in our laboratory. The results were compared with those of pure Pb in a 4 M H_2SO_4 solution. Tafel polarization and electrochemical impedance spectroscopy (EIS) techniques were used to study the electrochemical behaviour of the alloy in 4 M H_2SO_4.

Experimental

Material

A stock solution of 4 M H_2SO_4 acid (the acid used in the lead/acid battery) was prepared by dilution of the calculated volume of A.R. grade acid. Pb and Mg of high purity (99.999%) were used to prepare Pb-Mg alloys as disk electrodes (A = 1 cm^2) in a Gallenkamp muffle furnace, using evacuated closed silica tubes, at 603 K (330 ºC), for 20 min.
The melts were shaken every 5 min to ensure the homogeneity of the melting alloys. Finally, the melts were quenched in cold water (10 ºC), in order to obtain a

supersaturated solid solution. Four samples of Pb-Mg alloys with different Mg contents (0.5, 0.8, 1 and 1.5 % wt) were prepared with the same procedure.
The temperature, as well as Mg percentages, were chosen based on the phase diagram of Pb-Mg alloys (Fig. 1). The investigated alloys were analyzed using the Thermo Scientific Niton XL5 X-ray fluorescence spectrometer. For each alloy, the percentage of Pb and Mg was found in accordance with the percentage of the Pb and Mg mixture.

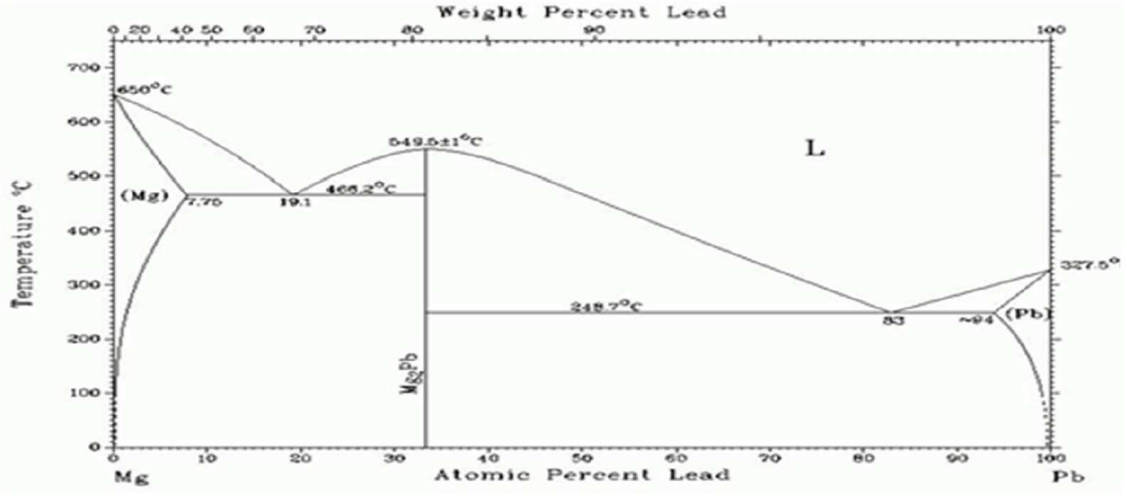

Figure 1. Phase diagram of Pb-Mg alloys.

The composition of lead with different contents of Mg is represented in Table 1.

Table 1. Chemical compositions of pure Pb and Pb-Mg samples.

Mg added (%)	Pb (%)	Mg (%)	Sn (%)	Si (%)	P (%)	Cr (%)	Al (%)	Zn (%)
0	99.890	-----	0.050	-----	0.058	0.002	-----	-----
0.5	99.498	0.500	0.001	0.000	-----	-----	0.001	-----
0.8	99.100	0.800	0.002	-----	0.093	0.0008	-----	0.004
1	98.893	1.000	0.002	0.086	0.010	0.009	-----	-----
1.5	98.447	1.500	-----	0.027	-----	0.0001	0.025	0.0008

Optical microscopy

The physical properties of the quenched solid solutions of lead alloys evolve at room temperature (25 ºC). The hardening mechanisms are continuous/discontinuous transformations.
In fact, this temperature corresponds to 0.5 Tf (alloy's melting temperature). We know that from 0.4 to 0.5 Tf, the alloy elements can diffuse. In the case where the kinetics of the discontinuous transformation is rapid at room temperature, we have used the original technique developed by Hilger [13], in order to be able to observe the structure before any transformation.
For our alloys, the sample was polished and soaked in a chemical solution consisting of one part of 30% H_2O_2 and three parts of glacial acetic acid. The solution temperature was -50 °C. The duration of the immersing process varied between 20 sec and 2 min, depending on the state of the sample. The chemical

polishing was followed by repeated chemical attacks/etching using a mixture of 100 mL distilled water, 25 g of citric acid and 10 g of ammonium molybdate.

Electrochemical measurements

For electrochemical measurements, a three-electrode conventional glass cell was used. The experiments were performed in a 250 mL volume borosilicate glass cell, using a Pt wire and a saturated calomel electrode (SCE) as auxiliary and reference electrodes, respectively. SCE tip was very close to the surface of the working electrode, to minimize the IR drop. All potentials given in this paper are referred to this reference electrode. A flat working electrode surface was obtained by mechanical polishing with emery papers of successively decreasing grain size (1200, 800 and 400). The working electrodes were rinsed with double-distilled water. The electrolyte was a 4 M H_2SO_4 solution. To remove any surface contamination and air-formed oxide, the working electrode was kept at -1.2 V (SCE), for 10 min, in the tested solution. Then, it was disconnected and shaken free of adsorbed hydrogen bubbles. The potentiodynamic polarization, with a scanning speed of 1 mV/s, began with a potential of -1.5 V, and ended with a potential of +2.3 V. The linear Tafel segments of the cathodic and anodic curves were extrapolated to the corrosion potential, to obtain the corrosion current densities (I_{corr}). Measurements were conducted at 298 K, 313 K, 333 K, and 353 K (25 ºC, 40 ºC, 60 ºC, and 80 ºC), for each investigated electrode.

The measurements of the electrochemical impedance spectroscopy have been carried out using a margin of frequency ranging from 100 kHz to 10 Hz, at the corrosion potential. For the analysis, we used the 10 VoltaLab model (PGZ100) device connected to an HP computer. The acquisition and processing of data were done using VoltaMaster 4 and OriginLab software.

Results and discussion

Optical microscopy

The first transformation began during the first sec of ageing at room temperature. The observations show a discontinuous transformation with fronts originating from the grain boundaries and sweeping quickly over the whole surface. Fig. 2 shows the regular progression of the transformation front in the bulk of the grain.

When two fronts from two different grains boundaries come together, a new stationary boundary is formed (b). The borders of the cells have a tendency to blur lightly behind the front. This phenomenon could be explained by a reorganization (partial homogenization) of the segregated elements on the boundaries of the solidification cells, during the passage of the transformation.

Micro-hardness

The hardness values of Pb and Pb-Mg alloys were measured by employing the Vickers micro-hardness test procedure with a Vickers pyramidal indentor. The Vickers hardness number is given by $HV = 0.185\ F/d^2$, where F is the applied load and d is the average diagonal length in millimeters. Each value was an average of, at least, three measurements determined on the surface of the specimens. The data

in Fig. 3 reveal a non-linear increment of the micro-hardness, with an increase in Mg content in the alloy. Noteworthy, the Pb-1.5%Mg alloy almost shows threefold micro-hardness values (14.6 HV), in comparison to those of pure Pb (5 HV). The micro-hardness of the Pb-Mg alloy not only depends on its chemical composition, but it is also significantly affected by the micro-structure array. One can conclude that the increase in micro-hardness with the increasing Mg alloying can be attributed to grain refinement, as previously shown in optical microscope results.

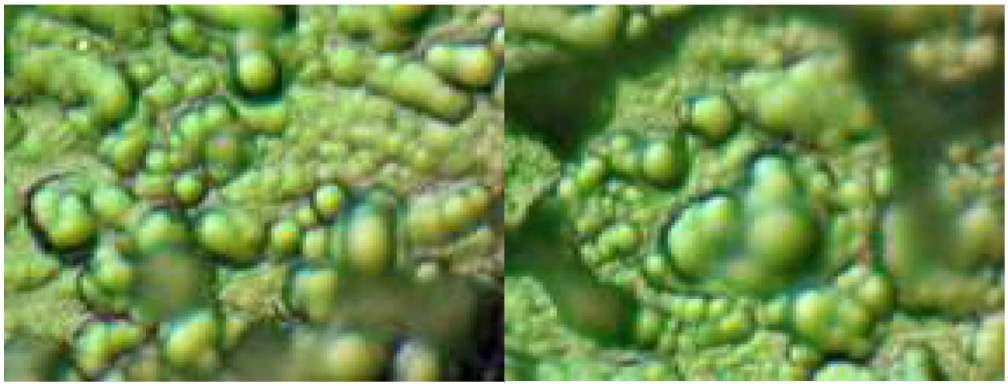

Figure 2. Microstructure of quenched cast Pb-1.5%Mg alloy at 25 °C. Visualization of the discontinuous transformation **(a)** after 1 hour **(b)**.and after 1 month

Accordingly, the existence of a certain percentage of Mg inside Pb micro-structure would lead to the improvement of its mechanical properties.

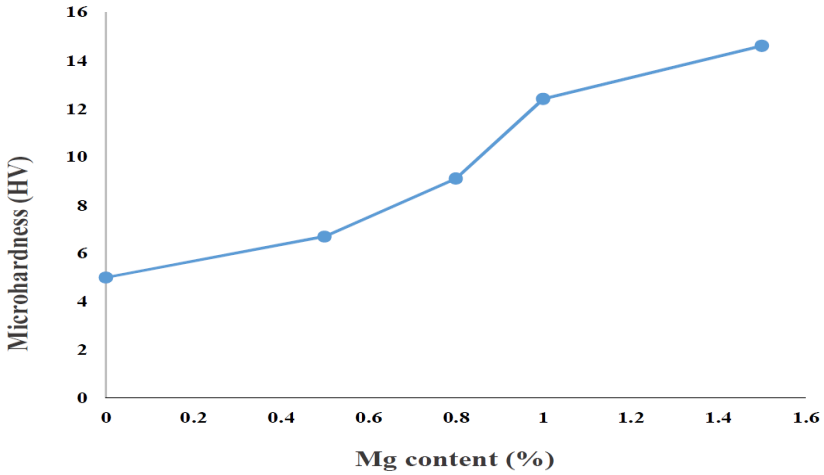

Figure 3. Variation of micro-hardness with magnesium in the specimen.

Electrochemical measurements

Effect of Mg concentration: Potentiodynamique polarization

Fig. 4 represents the experimental results from polarization curves of pure Pb and Pb-Mg alloys in 4 M H_2SO_4, with a scan rate of 1 mV/s, at 25°C (298 K). Corrosion parameters were calculated on the basis of cathodic and anodic potential vs current density characteristics in the Tafel potential region. The values of the corrosion current density (I_{corr}) for the samples were determined by extrapolation of the cathodic and anodic Tafel lines to corrosion potential (E_{corr1}) (Table 2).

There is a marked shift towards lower current densities (I_{corr}), in the case of the investigated Pb-Mg alloys, compared with those of pure Pb. However, these shifts were accompanied by a significant decrease in corrosion rates. These shifts were greater as Mg content was increasing. This indicated that Mg content in the alloy plays an important role in slowing down Pb corrosion rate. The two breaks observed in the anodic branch, at a more positive potential (at ≈450 mV/SCE), can be attributed to the formation of a thick layer of $PbSO_4$ and lead oxide, respectively, on the metal surface in this region. On the other hand, the negative shift in the corrosion potential (E_{corr}), with a simultaneous decrease in the corrosion rate of the investigated alloys, compared with that for pure Pb, can be ascribed to Pb-Mg phase formation (Fig.4).

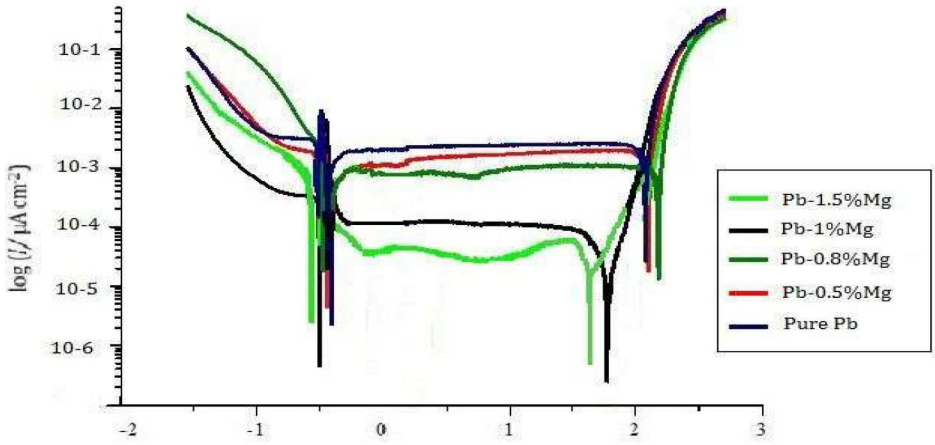

Figure 4. Polarization curves of Pure Pb and Pb-Mg alloys in 4 M H_2SO_4, at 25°C.

Table 2. Corrosion parameters obtained from Tafel Slopes extrapolation for pure Pb and Pb-Mg alloys in 4 M H_2SO_4, at 25°C.

Alloy	E_{corr1} (mV/SCE)	E_{corr2} (mV/SCE)	I_{corr} (µA/cm^2)	I_{pass} (µA/cm^2)	E_{tra} (mV/SCE)	Corrosion rate (mm/year)
pure Pb	-462	-458	349	374	2362	41.62
Pb-0.5%Mg	-471	-455	300	338	2425	30.14
Pb-0.8%Mg	-498	-470	274	301	2450	20.92
Pb-1%Mg	-500	-491	116	132	1851	8.02
Pb-1.5%Mg	-573	-510	59	82	1687	3.91

The shift of the alloy corrosion potential to a more negative direction, with the increase in Mg content, can be attributed to Mg potential, which is more negative than that of Pb.

In previously published researches [14], it was found that the alloying solid-solution phase on the alloy as a separated phase acts as cathodic site on the alloy surface. Therefore, we can assume that Mg presence as alloying element decreases the density of active sites on the alloy surface, compared with those of Pb.

Consequently, the alloy dissolution rate decreases in a H_2SO_4 solution, compared with that of pure Pb. This can explain the shift of E_{corr} towards more negative values in Pb-Mg alloys, compared to that of pure Pb.

As shown in Table 2, the corrosion current density (I_{corr}) of Pb-1.5%Mg is 59 µA/cm^2, while that for pure Pb is 349 µA/cm^2, at 25 °C. Thus, the addition of 1.5% of Mg to Pb reduced the corrosion rate by 83% (Fig. 5).
This inhibition efficiency (ŋ) was calculated by using the following equation:

$$\eta = \frac{CR - CR'}{CR} \times 100 \qquad (1)$$

where CR is the corrosion rate of pure Pb and CR' is the corrosion rate of Pb-Mg.
These results indicate that Mg addition leads to a significant increase in Pb corrosion resistance. This behaviour can be interpreted based on previous works [15] done on the corrosion of Pb, by assuming that Mg particles tend to be oriented towards the surface and stay that way during Pb dissolution. Since the dissolution of crystalline structures typically proceeds layer by layer along the steps, the formation of solid particles along the steps may have an effect of blocking the sites for the dissolution reaction [16]. This argument would be due to the result of I_{corr}, which showed that the corrosion rate (Table 3) decreases significantly with Mg addition.

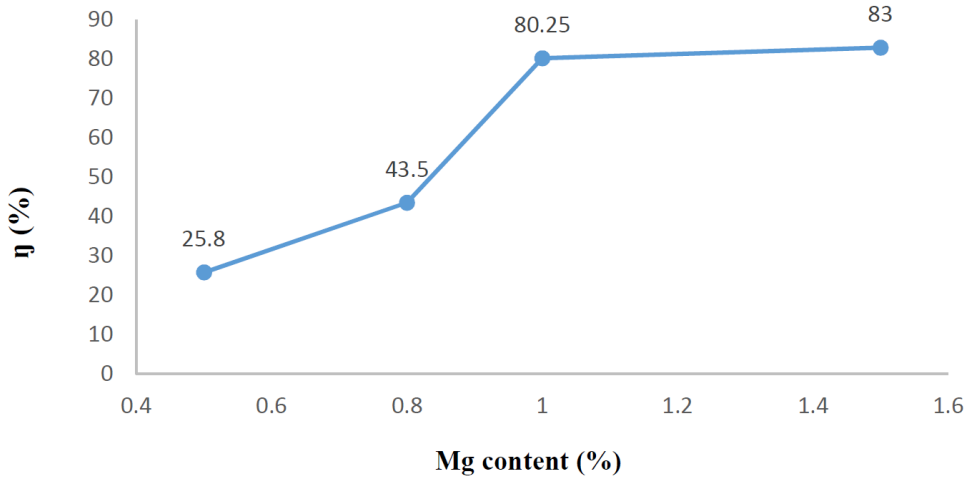

Figure 5. Relationship between Mg contents and the inhibition efficiency based on potentiodynamique polarization parameters.

We can also notice a decrease in I_{pass} with increasing Mg content. This can be explain by the fact that the formation of the two corrosion compounds ($PbSO_4$ and PbO) decreases, since Mg decreases Pb corrosion rate. Therefore, the size of the thick passive layer decreases by adding Mg, and I_{pass} decreases accordingly.
At the anodic potentials, the products of the corrosion (PbO and $PbSO_4$) are transformed into PbO_2 by a reaction with sulfuric acid.
This transformation is indicated by a peak of polarization characterized by a potential of transpassivation (E_{tra}) followed by an increasing current corresponding to oxygen evolution.
The results show that the addition of Mg up to 1.5% leads to a decrease in the E_{tra}, meaning that Mg tends to facilitate the transformation of $PbSO_4$ and PbO to PbO_2.

This indicates that the phenomenon of sulfation (formation and deposition of lead sulfate) will be reduced, in the case of Pb-Mg.

Effect of Mg content: Electrochemical Impedance Spectroscopy (EIS)

The impedance of the pure Pb and Pb-Mg alloys in a 4 M H_2SO_4 solution, at the steady state of open-circuit potential (E_{corr}), has been plotted, as shown in Fig. 6. An analysis for the impedance in the examined potential range was carried out. The data of the charge transfer resistance (R_t) and the capacity of the double layer (C_{dl}) were calculated using the Nyquist plot; the values are tabulated in Table 3.

Fig. 6 shows a comparison between the Nyquist plots of pure Pb and the Pb-Mg alloys (from 0.5 to 1.5%Mg), in a 4 M H_2SO_4 solution, at 25 ºC (298 K). The Nyquist plots were in the shape of a deformed semicircle. This indicates that the main reaction mechanism present on the double layer is the charge transfer mechanism, and that control of charged species by diffusion is absent [17-18]. Pure Pb and Pb-Mg alloys exhibited similar Nyquist plots in a 4 M H_2SO_4 solution. This means that the addition of Mg to Pb up to 1.5% does not change the main reaction mechanism on the metal surface. We can also notice that the increase in the semicircle diameter of all alloys is more than that of pure Pb. The maximum semicircle diameter is obtained in the case of Pb-1.5%Mg alloy. This behaviour exhibits very important results, showing that Mg content in the alloy plays an important role in decreasing the corrosion rate in a 4 M H_2SO_4 solution. Consequently, the corrosion resistance increases with the increase in Mg content in the alloy.

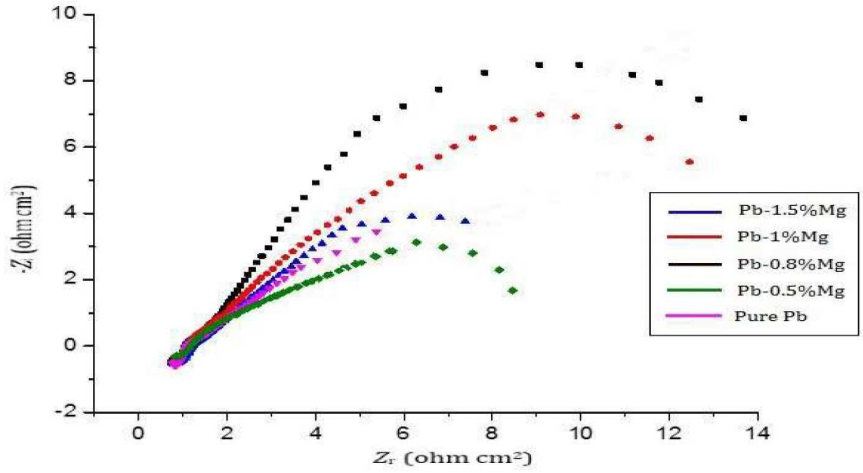

Figure 6. Nyquist plots for pure Pb and Pb-Mg alloys, in a 4 M H_2SO_4 solution, measured at E_{corr}, at 25 ºC.

Table 3 presents R_t and C_{dl} values, which are estimated from the impedance data at E_{corr} of Pb and Pb-Mg alloys. It is observed that R_t values increase, while C_{dl} values decrease with an increasing Mg content in the alloy. Accordingly, the results show that the corrosion resistance of Pb-Mg alloy is superior to that of pure Pb in 4 M H_2SO_4, and that Pb-1.5%Mg alloy gives higher corrosion resistance. The superior corrosion resistance observed for the investigated alloy, compared

with pure Pb, could be explained by the barrier protection mechanism theory, in which a barrier acts to prevent further attack by increasing the micro-hardness. This alloy is considered a stable alloy.

Table 3. Corrosion parameters obtained from Tafel plots for pure Pb and Pb-Mg alloys in 4 M H_2SO_4, at different temperatures.

Mg content	Temperature (K)	E_{corr1} (mV)	I_{corr} (µA/cm^2)	Corrosion rate (mm/year)
Pure Pb	**298**	-462	349	41.62
	318	-459	360	44.90
	338	-451	429	49.93
	358	-447	469	53.58
0.5%Mg	**298**	-471	300	30.14
	318	-462	314	33.54
	338	-454	326	35.75
	358	-447	337	40.85
0.8%Mg	**298**	-498	274	20.92
	318	-484	277	23.17
	338	-472	280	25.42
	358	-469	289	29.17
1%Mg	**298**	-500	116	08.02
	318	-483	119	09.22
	338	-474	128	10.84
	358	-466	130	11.98
1.5%Mg	**298**	-573	59	03.91
	318	-561	65	04.30
	338	-552	69	05.75
	358	-547	73	06.83

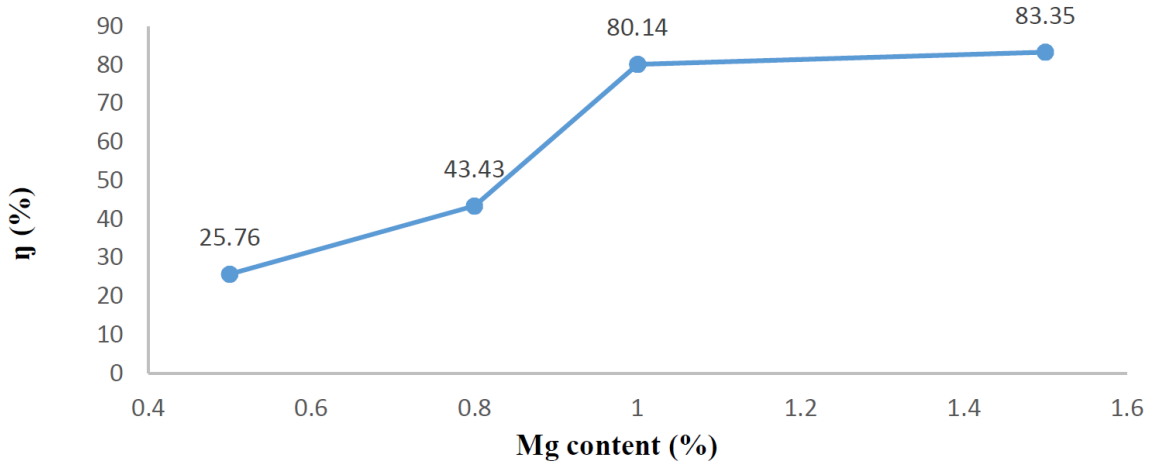

Figure 7. Relationship between Mg content and inhibition efficiency based on EIS parameters.

As previously found [19], once the lead alloy has been covered by the $PbSO_4$ layer, the attack on it is chiefly determined, at first, by the rate at which the Pb^{2+} ions diffuse from the $PbSO_4$ layer to the bulk solution; and then, upon complete saturation of the solution, by the much slower growth rate of the compact layer of

$PbSO_4$ precipitated on lead, protecting it from severe attack of sulfuric acid and, therefore, reducing its corrosion.
The corrosion inhibition efficiency was calculated from the EIS parameters, (Fig. 7), which are in accordance with those of the potentiodynamic polarization.

Effect of temperature on the corrosion of pure Pb and Pb-Mg alloys
Knowing that, inside a Pb-acid battery, temperature can achieve 358 K (80 ºC), we analysed the data to get electrochemical parameters at different temperatures (Table 4). These data show that the corrosion current density (I_{corr}) and the corrosion rate values increased with higher temperatures, for both pure Pb and Pb-Mg alloys.

Table 4. Activation energy (E_a) values in kJ/mol, for Pb and Pb-Mg alloys in 4 M H_2SO_4.

Mg content	Ea (kJ/mol)
Pure Pb	3.82
Pb-0.5%Mg	4.30
Pb-0.8%Mg	4.80
Pb-1%Mg	6.06
Pb-1.5%Mg	8.64

In an acidic solution, the logarithm of the corrosion rate is a linear function of 1/T (Arrhenius-type equation [20]. Fig. 8 is shown according to the Arrhenius plots for the corrosion of pure Pb and its investigated alloys, by plotting log CR (mm/year) against 1/T.

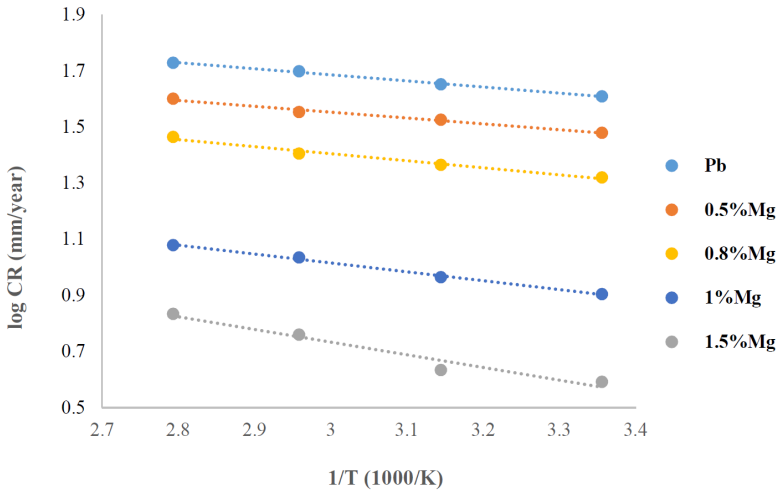

Figure 8. Arrhenius plots for corrosion of pure Pb and Pb-Mg alloys in 4 M H_2SO_4 using corrosion rate vs 1/T.

The activation energy for corrosion can be obtained by Arrhenius equation:

$$\log(CR) = \frac{-Ea}{2.303RT} + A \qquad (2)$$

where E_a is the activation energy of the pure Pb and Pb-Mg alloys dissolution reaction, R is the general gas constant and A is the Arrhenius pre-exponential

factor. In all cases studied, a plot of the logarithm of corrosion current density vs 1/T resulted in straight lines, with a slope $-E_a/2.303R$. The resulted plots are shown in Fig. 8, and all calculated activation energies for the pure Pb and Pb-Mg alloys are given in Table 4.

Fig. 8 and Table 4 show that the E_a values of Pb-Mg alloys, in a 4 M H_2SO_4 solution, are much higher than that of pure Pb. This behaviour is attributed to the presence of a solid-solution phase which enhanced the activation energy barrier of the corrosion, thus reducing the corrosion rate of the alloy [21]. The higher E_a values determined for the alloys can be ascribed to the lower active sites and/or to a decrease in anodic to cathodic area ratio [22]. The presence of the single phase in the alloy not only makes a lower rate of the hydrogen evolution reaction, but also inhibits it. It is claimed in the literature that the formation of this single phase in the alloy provides the best protection with the lowest self-corrosion rate [23]. These E_a values support this trend of the corrosion rate obtained for Pb and its studied alloys, as mentioned before.

Conclusions

In this framework, the effect of Mg content on both micro-hardness and crystallite structure of the Pb-Mg alloy was investigated. The corrosion resistance of the mentioned alloys in a H_2SO_4 solution was studied by potentiodynamic polarization, as well as by EIS. Several conclusions can be extracted from these investigations:

- The micro-hardness increases, while the crystallite size decreases with increasing magnesium content in the alloy. This trend is attributed to the refinement of the crystalline size and lattice distortion by the addition of magnesium. Pb-Mg alloy is much harder and resistant to mechanical shocks than pure Pb.
- Pb-Mg alloys have good corrosion resistance in a 4 M H_2SO_4 solution, compared with that of pure Pb. Addition of 1.5% in weight of Mg led to a decrease in the corrosion rate by 83%. This behavior can be interpreted on the basis that the solute content tends to refine the micro-structure array. Since this alloy is very stable, the passive layer formed with $PbSO_4$ and PbO is blocking the sites of dissolution reactions.
- Potentiodynamique polarization results showed a corrosion potential (E_{corr}) towards negative values and a significant reduction of the corrosion current density (I_{corr}). This means that the corrosion rate decreased and that the corrosion resistant of Pb-Mg alloys, compared to that of pure Pb, is higher.
- The results of both Tafel plots extrapolation and EIS measurements exhibited the same trend that the corrosion rate on the alloy surface is less significant compared with that on the surface of pure Pb, and that Pb-1.5%Mg yielded the best resistance to corrosion in 4 M H_2SO_4.
- The corrosion rate of lead and its investigated alloys increases with an increasing temperature, while its effect seems to be more pronounced for alloys than that for lead. The activation energy values of the pure lead and its studied alloys were calculated and compared.

References

1. Felder A, Prengaman RD. Lead alloys for permanent anodes in the nonferrous metals industry. J Metal. 2006;58:28-31.
2. Bullock KR. The Effect of Phosphoric Acid on the Positive Electrode in the Lead-Acid Battery: II . Constant Potential Corrosion Studies. J Electrochem Soc. 1979;126:360.
3. Meissner E. Large lead/acid batteries for frequency regulation, load levelling and solar power applications. J Power Sources. 1997;67:135-150.
4. Li DG, Zhou GS, Zhang J, et al. Investigation on characteristics of anodic film formed on PbCaSnCe alloy in sulfuric acid solution. Electrochim Acta. 2007;52: 2146.
5. Garche J, Döring H, Wiesener L. Influence of phosphoric acid on both the electrochemistry and the operating behaviour of the lead/acid system. J Power Sources. 1991;33:213-220.
6. Abd El-Rahman HA, Salih SA, Abd El-Wahab AM. Effect of phosphoric acid on the performance of low antimony grid of Pb-acid cell under constant current charging and discharging. Mater Sci. Eng Tech. 2011;42:784.
7. Osório WR, Peixoto C, Garcia A. Electrochemical corrosion of Pb-1 wt% Sn and Pb-2.5 wt% Sn alloys for lead-acid battery applications. J Power Sources. 2009;194:1120.
8. Čekerevac MI, Romhanji E, Cvijović Z, et al. The influence of tin and silver as microstructure modifiers on the corrosion rate of Pb-Ca alloys in sulfuric acid solutions. Mater Corros. 2010;61:51.
9. Prengaman RD. Challenges from corrosion-resistant grid alloys in lead acid battery manufacturing. J Power Sources. 2001;95:224.
10. Albert L, Chabrol A, Torcheux L, et al. Improved lead alloys for lead/acid positive grids in electric-vehicle applications. J Power Sources. 1997;67:257.
11. Khatbi S, Gouale Y, Lamiri A, et al. Improving the Corrosion Resistance of Lead in H2SO4 4 M by the Addition of Phosphoric and Phosphonic Compounds for Lead Grid Batteries. Port Electrochim Acta. 2016;34:383.
12. Khatbi S, Gouale Y, Lamiri A, et al. Electrochemical and Metallurgical Behavior of Lead-Aluminum Casting Alloys as Grids for Lead-Acid Batteries. Port Electrochim Acta. 2018;36:133.
13. Hilger JP, Boulahrouf JH. Observation of the first stages of discontinuous transformation in Pb-Ca alloys used for lead batteries. Mater Character. 1990 ;24:159.
14. El-Sayed A, Essalam MM, Hossnia S, et al. Metal Mater Trans A. 1995;46:176.
15. Refaey SAM, Taha F, Hasanin THA. Passivation and pitting corrosion of nanostructured Sn-Ni alloy in NaCl solutions. Electrochim Acta. 2006;51:2942.
16. Hongxia L, Zhilin W. Adv Mater Res. 2013;721:104.
17. Morakchi K, Hamel A, Zazoua A. J Ren Ener. 2008;11:362.
18. Larabi L, Harek Y, Traisnel M. Synergistic influence of poly(4-vinylpyridine) and potassium iodide on inhibition of corrosion of mild steel in 1M HCl. J Appl Electrochem. 2004;34:833.
19. Gonzulez JA, Fullru J, Feliu S. Wcrk Korros. 1975;26:10.
20. Kiani MA, Mousavi MF, Ghasemi S, et al. Inhibitory effect of some amino acids on corrosion of Pb-Ca-Sn alloy in sulfuric acid solution .Corros Sci. 2008;50:1035
21 Mohran HS, El-Sayed A, Abd El-Lateef HM. Anodic behavior of tin, indium, and tin-indium alloys in oxalic acid solution. J Solid State Electrochem. 2009;13:1279.
22. El-Sayed A, Mohran HS, Abd El-Lateef HM. Effect of minor nickel alloying with zinc on the electrochemical and corrosion behavior of zinc in alkaline solution. J Power Sources. 2010;195:6924.
23. Fekry AM, Gasser AA, Ameer MM. Corrosion protection of mild steel by polyvinylsilsesquioxanes coatings in 3% NaCl solution. J Appl Electrochem. 2010;40:739.